Experimental Evaluation of Non-Coherent MIMO Grassmannian Signaling Schemes

Jacobo Fanjul*, Jesús Ibáñez, Ignacio Santamaria, and Carlos Loucera

Department of Communications Engineering, University of Cantabria, 39005 Santander, Spain
{fanjulj,jesus.ibanez,i.santamaria,carlos.loucera}@unican.es

Abstract. In this paper, we present an over-the-air (OTA) performance analysis of Grassmannian signaling strategies in an orthogonal frequency-division multiplexing (OFDM) single-user multiple-input multiple-output (SU-MIMO) scenario. Specifically, we compare the Grassmannian signaling technique to the differential Alamouti scheme and a novel space-time non-coherent scheme recently proposed in the context of 5G. As a performance benchmark we include in the comparison the coherent Alamouti scheme. We study the practical impairments associated to frequency synchronization mismatches (frequency offsets), as well as the effects of time-varying channels for different spectral efficiencies. The experimental results show that non-coherent techniques are more robust to the aforementioned impairments than the coherent Alamouti approach, while Grassmannian methods are close to the differential Alamouti scheme with 2 transmit antennas.

Keywords: Non-coherent communications; Grassmannian signaling; MIMO testbed; OFDM; Over-the-air (OTA) experiments.

1 Introduction

The vast majority of wireless communications systems rely on the use of channel state information (CSI), at least at the receiver end. However, some scenarios might present short coherence times due, for instance, to large Doppler spreads associated to communications with terminals mounted in high-speed vehicles. For very fast time-varying scenarios, channel estimation might not be even feasible. Even if accurate channel estimates can be obtained in fast fading scenarios, the associated overhead implies a significant reduction in terms of throughput. In the context of 5G, the concept of massive multiple-input multiple-output (MIMO) is attracting significant research efforts [7]. Considering the large amount of antennas and, consequently, the associated channel state information to be handled in

these scenarios, non-coherent strategies are receiving renewed interest for massive MIMO.

Since the first differential coding schemes for phase-shift keying (PSK) systems were proposed for systems using a single transmit antenna [16], several non-coherent transmission techniques have been developed for MIMO systems. A remarkable approach is the differential Alamouti scheme presented in [15], which retains the nice properties of the popular Alamouti [2] with only a 3 dB loss with respect to the coherent case. This scheme was later generalized to other differential space-time block codes (DSTBC) with more than two transmit antennas in [9], but with a reduction in rate. The design of a rate-2 differential STBC was described in [1].

The study of the capacity of non-coherent MIMO systems in block fading channel models was considered in [12], where the structure of the capacity achieving input distribution was characterized (the capacity achieving transmitted signals are isotropically distributed unitary matrices). Shortly afterwards, the use of differential space-time modulations was proposed in [6], [8]. Following a similar line, Zheng and Tse presented in [17] the Grassmannian signaling technique, which relies on the fact that the space spanned by the transmitted matrices is invariant to the channel matrix. In this way, the design of optimal transmit matrices for non-coherent schemes can be posed as a sphere packing problem on the Grassmann manifold. To solve this problem, an alternating projection algorithm is provided in [4]. Further advances on Grassmannian constellation design and detection are presented in [5],[3].

In the experimental area, only a few works have been conducted to evaluate the performance of differential STBC schemes over real scenarios (see [13]). However, the experimental performance evaluation of Grassmann-based signaling schemes using over-the-air (OTA) transmissions is still lacking. In this work, we attempt to fill this gap and present an experimental comparison between Grassmannian-based signaling schemes and other well-known non-coherent techniques, namely the differential Alamouti method in [15] and the PSK-based ST scheme proposed in [10].

1.1   Notation

Uppercase and lowercase boldface letters will be used for matrices and column vectors, respectively. $(\cdot)^T$ will represent transpose, whereas $(\cdot)^H$ denotes conjugate transpose (Hermitian). Additionally, $\mathbf{I}$ stands for the identity matrix, $\text{Tr}(\cdot)$ represents the trace operator and $\text{vec}(\cdot)$ is used for vectorization. Finally, the notation $\mathbb{G}(T, M)$ will be used to represent the Grassmann manifold containing all subspaces of dimension M in a T-dimensional ambient space.

2   Grassmannian Signaling overview

In this section, we present a brief description of Grassmannian signaling for MIMO non-coherent transmissions. Given a transmitter with M antennas, a

receiver equipped with N antennas, and a coherence time T within which the channel remains constant, the received signal $\mathbf{Y} \in \mathbb{C}^{N \times d}$ is given by

$$\mathbf{Y} = \mathbf{H}\mathbf{X} + \mathbf{W}, \tag{1}$$

where $\mathbf{X} \in \mathbb{C}^{M \times d}$ is the transmitted signal over d time slots, $\mathbf{H} \in \mathbb{C}^{N \times M}$ is the channel matrix, and $\mathbf{W}$ denotes additive white Gaussian noise (AWGN). Also, notice that time indexes have been omitted in this general signal model for the sake of notational simplicity.

It was shown in [12] [6] [8] that at high-SNR the capacity of a non-coherent block-fading MIMO channel is achieved transmitting isotropically-distributed unitary matrices provided that $T \geq \min(M, N) + M$. The resulting capacity achieving approach has a nice geometric interpretation as a Grassmannian signaling scheme [17], where the transmitted signals are K-dimensional subspaces in $\mathbb{C}^T$, with $K = \min(M, N, \lfloor \frac{T}{2} \rfloor)$. It is also worth mentioning that, as stated in [17], no additional benefit in terms of capacity can be attained by increasing either M or N beyond $T/2$.

The main intuition behind Grassmannian signaling is that the received signal $\mathbf{Y}$ spans the same row space as the transmitted signal $\mathbf{X}$ for any nonsingular channel $\mathbf{H}$. For a given configuration with $M \leq N$ and $T \geq 2M$, we can send up to $M(T - M)$ information streams over T time slots by transmitting subspaces from a codebook $\mathcal{X}$ formed by subspaces in the Grassman manifold $\mathbb{G}(T, M)$ [1]. Consider that the transmitted subspace is $\mathbf{X}[n] = \mathbf{X}_i$; then, at the receiver side the optimal decoding rule is given by the generalized likelihood ratio test (GLRT)

$$\hat{\mathbf{X}}_i = \arg \max_{X_j \in \mathcal{X}} \left(\operatorname{Tr} \left(\mathbf{Y}\mathbf{X}_j^H \mathbf{X}_j \mathbf{Y}^H \right) \right), \tag{2}$$

with a complexity that grows exponentially with the block-length T.

3   Frame format and experimental setup

This section describes the indoor MIMO testbed that has been used to conduct the over-the-air experiments, as well as the frame format. Fig. 1 shows the experimental set-up, whose main points are the following:

- The link is a 2×2 MIMO system, and the Tx-Rx distance is approximately 2 meters.
- Both transmitter and receiver functionalities have been implemented with Universal Software Radio Peripheral (USRP) B210 software-defined radio (SDR) devices, which are equipped with Analog Devices AD9361 single-chip direct-conversion transceivers and Spartan6 XC6SLX150 FPGA.

---

[1] The (complex) dimension of the Grassmann manifold $\mathbb{G}(T, M)$ is $\dim(\mathbb{G}(T, M)) = M(T - M)$, and therefore the multiplexing gain or pre-log factor of the system is $M(1 - M/T)$.
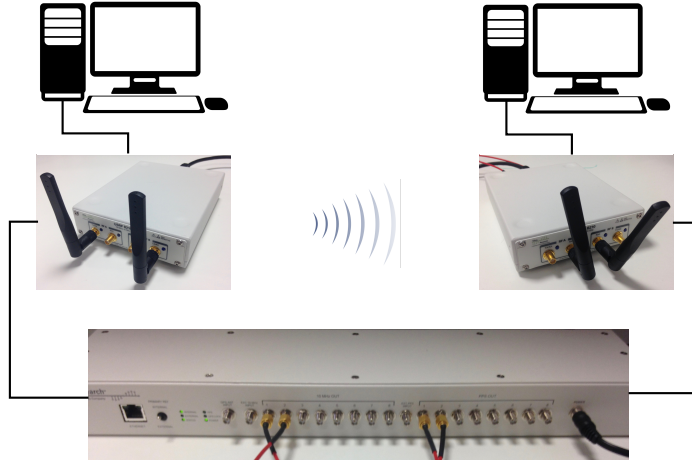
Fig. 1. Experimental set-up. The distance between transmitter and receiver is approximately 2 meters.

Standard 802.11a header	Coherent training	Alamouti OFDM symbols	2 + diff. Alamouti OFDM symbols	Grass. short T OFDM symbols	Grass. long T OFDM symbols	Space-time UL OFDM symbols

Fig. 2. Frame format used in our experiments.

- Additionally, for those experiments requiring precise frequency synchronization, we use the Ettus OctoClock module, which provides a high-accuracy timing reference signal for up to eight nodes.
- Both transmitter and receiver have been configured and controlled using the GTIS software provided by the GTEC Group from University of A Coruña, Spain.

Using this set-up, we transmit frames with the format shown in Fig. 2. Since we consider broadband transmissions over frequency-selective channels, we use the OFDM-based IEEE 802.11a wireless local area network (WLAN) physical-layer standard to construct the frames. Each subcarrier can be viewed as a 2×2 MIMO channel, and the non-coherent schemes are encoded over T consecutive OFDM symbols. The initial block is the common header for 802.11a transmissions (short-training symbols for frame detection and long-training symbols for coarse frequency estimation).

We include in the comparison the coherent Alamouti scheme, which is the first payload data after the channel estimation stage (needed only for this scheme). Then, we append in the frame a number of OFDM symbols for the differential Alamouti, the Grassmannian signaling scheme with two different ambient space configurations, and finally, the non-coherent scheme in [10].

The schemes under study have been evaluated for two different spectral efficiencies, namely, $\eta = 1$ and $\eta = 2$ bps/Hz, which are achieved as follows:

- For $\eta = 1$ bps/Hz, Alamouti-based schemes rely on BPSK symbols. For the Grassmannian signaling we transmit 2-dimensional subspaces in ambient spaces of dimension $T_{short} = 4$ and $T_{\ell ong} = 6$. In order to accommodate the corresponding number of bits within each subspace, 16 and 64-element codebooks are used for $T_{short} = 4$ and $T_{\ell ong} = 6$, respectively. For the PSK-based non-coherent scheme, we take $L = 4$-symbol codebooks.
- For spectral efficiency $\eta = 2$ bps/Hz, QPSK constellations are transmitted for both coherent and differential Alamouti techniques, the Grassmannian codewords are drawn from 256-element $\mathbb{G}(4, 2)$ and 1024-element $\mathbb{G}(5, 2)$ codebooks, respectively. For the last scheme, an $L = 16$-symbol constellation is used.
- The Grassmannian codebooks used throughout this work have been designed by means of the alternating projection algorithm in [4].

For each experiment, the previous sequences have been transmitted over 48 data subcarriers in the 2.487 GHz band, and spanning a total bandwidth of 8MHz.

4 Experimental Results

In this section we evaluate the performance of the non-coherent MIMO schemes in realistic wireless scenarios by means of OTA experiments. We have carried out several measurement campaigns to analyze the performance degradation caused by frequency estimation offsets as well as the impact of time-varying channels. For each experiment, the results of 1000 independent transmissions at different transmit power levels have been averaged.

4.1 Frequency offset

For each spectral efficiency ($\eta = 1$ and $\eta = 2$), we made 1000 OTA experiments with two different configurations:

- A static scenario (coherence time much longer than the OFDM symbol duration) that uses an external frequency synchronization reference signal generated by an OctoClock device. This configuration is associated to the solid lines in Figs. 3 and 4.
- The same static scenario, but removing the high-accuracy timing reference signal. In this case, the frequency offset has been estimated using the long training symbols (LTS) included in the 802.11a standard. Dashed lines in Figs. 3 and 4 represent the results for this scenario.

The aim of this measurement campaign is to determine how a given frequency offset impacts the different transmission techniques. Figures 3 and 4 show the
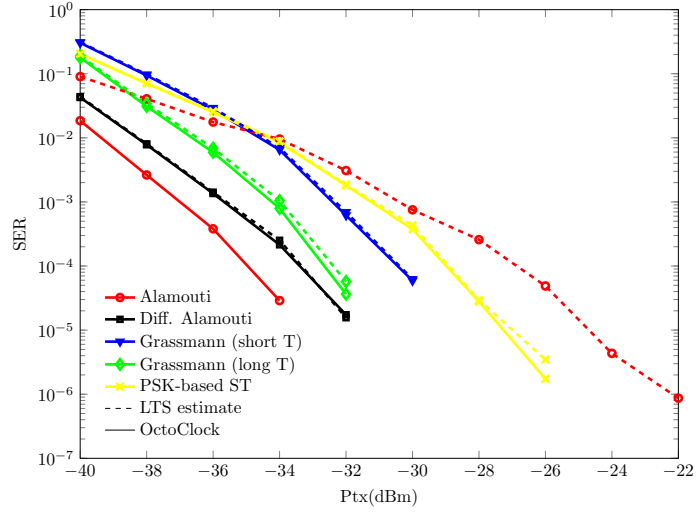
Fig. 3. SER for $\eta = 1$ bps/Hz with different freq. sync. approaches.
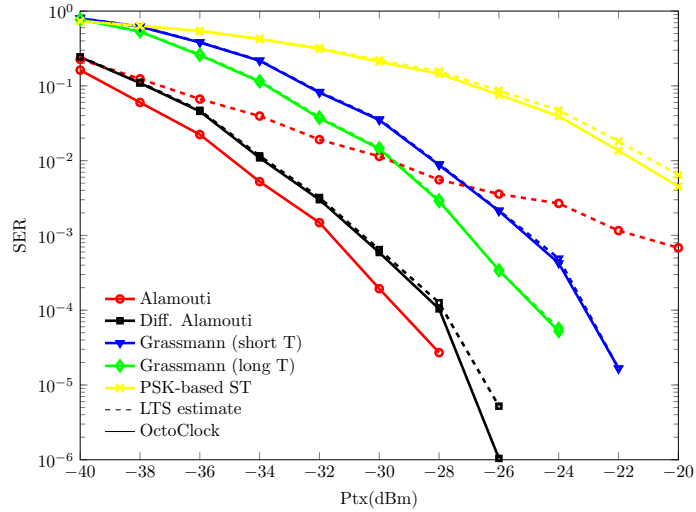
Fig. 4. SER for $\eta = 2$ bps/Hz with different freq. sync. approaches.

symbol error rate (SER) curves for spectral efficiencies $\eta = 1$ bps/Hz and $\eta = 2$ bps/Hz, respectively. As expected, the MIMO non-coherent schemes are significantly more robust to frequency synchronization errors than the coherent Alamouti approach. For the coherent Alamouti scheme, the offset provokes a rotation of the data symbols with respect to the channel estimate obtained from the training preamble, which in turn increases the SER especially for those

symbols located at the end of the coherent packet. On the other hand, for the non-coherent schemes the effect of the frequency offset is limited to the length of a codeword and it does not accumulate with time. In particular, the frequency offset effect is restricted to $T = 4$ OFDM symbols for the differential Alamouti (2 consecutive ST codewords), either T_{short} or $T_{\ell ong}$ OFDM symbols for the 2 Grassmanian signaling schemes under comparison, and only $T = 2$ OFDM symbols for the PSK-based non-coherent scheme. Therefore, the performance degradation due to frequency offsets is much more limited.

Turning now our attention to the comparison among the different non-coherent schemes, we observe that the PSK-based scheme in [10] provides the poorest performance, probably due to the fact that the method does not optimize the pairwise distance between ST codewords. Nevertheless, this method requires a coherence time of only $T = 2$ OFDM symbols, whereas the differential Alamouti requires the channel to remain constant for 2 consecutive blocks ($T = 4$), and for the Grassmannian signaling scheme it has to remain constant during the selected ambient space dimension (either $T = 4$ or $T = 6$ for $\eta = 1$ bps/Hz).

Regarding the Grassmannian signaling scheme, it can be observed that the behaviour improves when the ambient space dimension, T, increases. This is in agreement with theoretical works in [17, 11], which indicate that the performance of this non-coherent technique approaches the coherent capacity as the coherence time, T, tends to infinity (static channel).

Finally, it can be concluded from the figures that the best performing method is the differential Alamouti scheme. However, we can notice that the gap between the Grassmannian approaches and the differential Alamouti scheme is decreased when we reduce the spectral efficiency. This fact could be related to the number of elements in each codebook. Recall that, for spectral efficiencies $\eta = 1$ bps/Hz and $\eta = 2$ bps/Hz, the differential Alamouti builds on BPSK and QPSK constellations, respectively; whereas the Grasmannian signaling with $T_{\ell ong}$ uses 64 and 1024-element codebooks, respectively. Obviously, for a given ambient dimension a lower number of codewords allows us to increase the minimum distance between symbols and the codebook optimization is easier. Finally, it is worth mentioning that unlike the differential Alamouti, which is limited to 2 transmit antennas, Grassmannian signaling schemes can be applied to more general antenna configurations.

4.2 Time-varying channels

In this section, we evaluate the performance of the MIMO non-coherent schemes in fast-fading channels that arise in high-mobility wireless communications. In general, experimental evaluation of wireless technologies in high-mobility scenarios requires expensive equipment and sophisticated software processing [14]. To avoid these costs, in this work we emulate the fast-fading process at the transmitter side, and transmit frames filtered with time-varying channels generated with different Doppler spreads.

To focus only on the time selectivity of the channel, for this set of experiments we use an external clock to ensure frequency synchronization between the nodes. The frame format is the same as in Section 4.1, and we consider two different
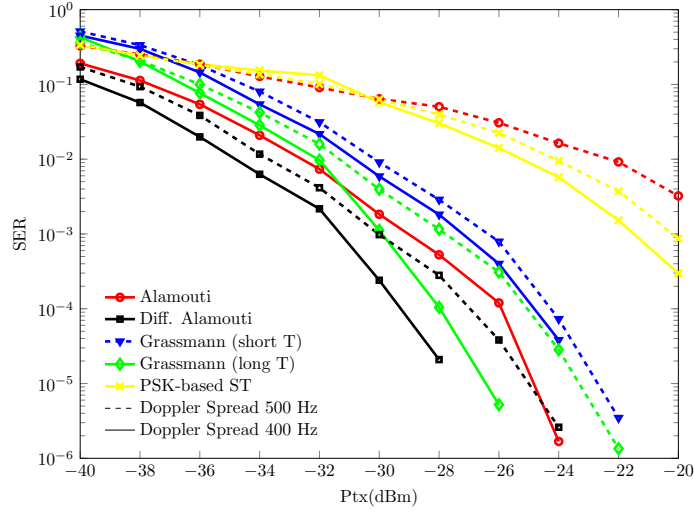
Fig. 5. SER for $\eta = 1$ bps/Hz and different Doppler spreads.
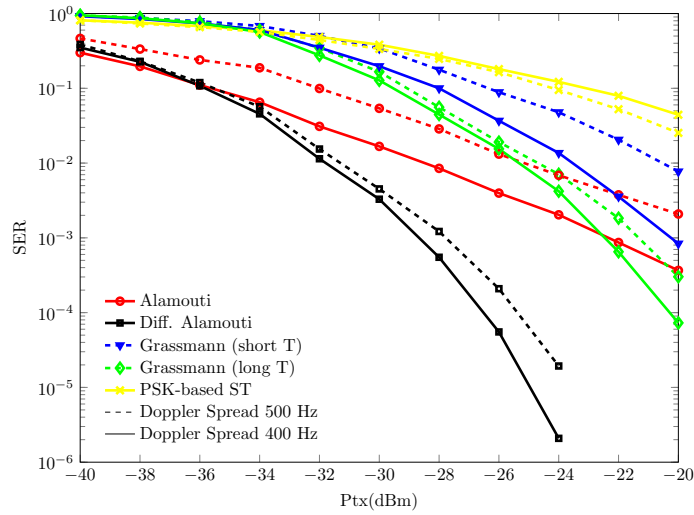
Fig. 6. SER for $\eta = 2$ bps/Hz and different Doppler spreads.

Doppler spreads: 400 Hz and 500 Hz. The SER curves for the schemes under comparison for $\eta = 1$ bps/Hz and $\eta = 2$ bps/Hz are presented in Figs. 5 and 6, respectively.

As observed in both figures, with the exception of the scheme in [10], non-coherent techniques are also more robust in fast-fading channels than the coherent scheme. Again, the best performing non-coherent scheme is the differential

Alamouti, especially for $\eta = 2$ bps/Hz. Remember also that the differential Alamouti scheme has a very simple optimal decoding rule in comparison to the GLRT detector used for the Grassmanian signaling scheme, whose complexity is exponential in T. Regarding the Grassmaniann signaling schemes, one would expect that increasing the Doppler spread would be more harmful for the scheme with higher ambient dimension T. However, Figs. 5 and 6 show that the codebook size (i.e., the spectral efficiency) also plays an important role here. This aspect requires further theoretical analysis and will be considered in a future work.

5 Conclusion

In this work, we have presented an experimental evaluation of 3 different non-coherent techniques in a wireless 2×2 MIMO-OFDM scenario. In particular, we have compared the performance of the subspace-based signaling technique to the differential Alamouti scheme and a recently proposed non-coherent scheme that uses PSK modulations. We have focused our study in two aspects of practical importance: i) the impact of frequency offsets between transmitter and receiver, and ii) the performance of these schemes under fast-fading (emulated) channels. While all non-coherent schemes are clearly more robust than the coherent Alamouti scheme under frequency offsets and time-selective channels, the differential Alamouti scheme seems to be the best performing non-coherent technique. Our study also showed that for the Grasmannian signaling scheme there are some interesting trade-offs between the ambient space dimension (number of channel uses over which the channel should remain constant) and the spectral efficiency (codebook size) that require further theoretical study. Also, it might be of interest to extend this experimental study to scenarios with more transmit antennas, for which existing DSTBC schemes have a penalty in rate [9].

References

1. Al-Dhahir, N.: A new high-rate differential space-time block coding scheme. IEEE Comm. Letters 11(11), 540–542 (2003)
2. Alamouti, S.: A simple transmitter diversity scheme for wireless communications. IEEE J. Select. Areas Comm. 16, 1451–1458 (Oct 1998)
3. Beko, M., Xavier, J., Barroso, V.A.N.: Noncoherent communication in multiple-antenna systems: receiver design and codebook construction. IEEE Trans. on Signal Proc. 55(12), 5703–5715 (2007)
4. Dhillon, I.S., Heath, R.W., Strohmer, T., Tropp, J.A.: Constructing packings in grassmannian manifolds via alternating projection. Exper. Math. 17(1), 9–35 (2008)
5. Gohary, R.H., Davidson, T.N.: Noncoherent mimo communication: Grassmannian constellations and efficient detection. IEEE Trans. on Inf. Theory 55(3), 1176–1205 (Feb 2009)
6. Hochwald, B.M., Sweldens, W.: Differential unitary space time modulation. IEEE Trans. on Comm. 48, 2041–2052 (2000)
7. Hoydis, J., Hosseini, K., Brink, S.t., Debbah, M.: Making smart use of excess antennas: Massive MIMO, Small Cells, and TDD. Bell Labs Technical Journal 18(2), 5–21 (2013), http://dx.doi.org/10.1002/bltj.21602

8. Hughes, B.: Differential space-time modulation. IEEE Trans. on Inf. Theory 46(7), 2567–2578 (2000)
9. Jafarkhani, H., Tarok, V.: Multiple transmit antenna differential detection from generalized orthogonal designs. IEEE Trans. on Inf. Theory 47(6), 2626–2631 (2001)
10. Li, G., Gong, F.: Space-time uplink transmission in non-coherent systems with receiver having massive antennas. IEEE Comm. Letters PP(99) (Dec 2016)
11. Li, Y., Nosratinia, A.: Product superposition for MIMO broadcast channels. IEEE Trans. on Inf. Theory 58(11), 6839–6852 (Nov 2012)
12. Marzetta, T.L., Hochwald, B.M.: Capacity of a mobile multiple-antenna communication link in Rayleigh flat fading. IEEE Trans. on Inf. Theory 45(1), 139–157 (1999)
13. Ramírez, D., *et al*: A comparative study of STBC transmissions at 2.4 GHz over indoor channels using a 2x2 MIMO testbed. Wireless Communications and Mobile Computing pp. 1149–1164 (Oct 2007)
14. Suárez-Casal, P., Rodríguez-Piñeiro, J., García-Naya, J.A., Castedo, L.: Experimental evaluation of the WiMAX downlink physical layer in high-mobility scenarios. EURASIP Journal on Wireless Communications and Networking (109) (2015)
15. Tarokh, V., Jafarkhani, H.: A differential detection scheme for transmit diversity. IEEE J. Select. Areas Comm. 18(7), 1169–1174 (Jul 2000)
16. Weber, W.: Differential encoding for multiple amplitude and phase shift keying systems. IEEE Trans. on Comm. 26(3), 385–391 (Jan 1978)
17. Zheng, L., Tse, D.N.: Communication on the Grassmannian manifold: A geometric approach to the noncoherent multiple-antenna channel. IEEE Trans. on Inf. Theory 48(2), 359–383 (Feb 2002)